FERMILAB-CONF-24-0669-AD
15th International Particle Accelerator Conference,Nashville, TN JACoW Publishing
ISBN: 978-3-95450-247-9 ISSN: 2673-5490 doi: 10.18429/JACoW-IPAC2024-WEPR48

MEASUREMENT OF STABILITY DIAGRAMS IN THE IOTA RING AT FERMILAB*

M.K. Duncan†, Y.-K. Kim, The University of Chicago, Chicago, U.S.
R. Ainsworth, N. Eddy, Fermi National Accelerator Laboratory, Batavia, U.S.
O. Mohsen, Argonne National Laboratory, Lemont, U.S.

Abstract

Nonlinear focusing elements enhance the stability of particle beams in high-energy colliders through Landau Damping (LD), by means of the tune spread introduced. Here we discuss an experiment at Fermilab's Integrable Optics Test Accelerator (IOTA) which investigates the influence of nonlinear focusing elements, such as octupoles, on the beam's transverse stability. In this experiment, we employ an anti-damper, an active transverse feedback system, as a controlled mechanism to induce coherent beam instability. By utilizing the anti-damper we can examine the impact of a nonlinear focusing element on the beam's transverse stability. The stability diagram, a tool used to determine the system's stability, is measured using a recently demonstrated method at the LHC. The experiment at IOTA adds insight towards this stability diagram measurement method by supplying a reduced machine impedance to investigate the machine impedance's effect on the stability diagram, as well as by aiming to map out the full stability diagram by using a large phase range of the anti-damper. From this experiment in IOTA, we present the first results of stability diagram analysis with high octupole current.

MOTIVATION

A challenge faced by many particle accelerators is maintaining high beam intensity. Major factors limiting beam intensity include collective instabilities which not only reduce the intensity but produce losses, irradiate components, and produce additional negative effects.

In the experiment at the Integrable Optics Test Acceleartor (IOTA) at Fermilab, we approach the challenge of beam intensity by studying beam stability. IOTA is an easily reconfigurable 40 m storage ring designed to run both electrons and protons at energies of 150MeV and 2.5MeV, respectively. This experiment is currently dedicated for when electrons are circulating in the ring.

The phenomena we study to understand beam stability is Landau Damping (LD). In accelerators, LD is the effect which damps collective oscillation modes and acts as a defense against collective instabilities. It depends on the spread of particle betatron frequencies and works through the energy transfer between coherent and incoherent oscillation modes at the same frequency [1]. A detailed knowledge of the strength of LD in particle accelerators is essential for predictions of beam stability, where studies of LD are often approached via Stability Diagram (SD) Theory.

* Work supported by Fermilab, UChicago, and the NSF GRFP
† mbossard@uchicago.edu

SD Theory depends on the dispersion relation between the beam's coherent tune shift from an external excitation and the tune of the mode. The dispersion relation for a coherent vertical degree of freedom is shown in Eq. (1):

$$\Delta\omega = -1/\int \frac{J_y \partial F/\partial J_y}{\Omega + \delta\omega(J_x, J_y) + i\sigma} dJ_x dJ_y \qquad (1)$$

Where $\Delta\omega$ is the coherent tune shift, Ω is the tune of the mode, J_y is the action in the y-plane, J_x is the action in the x-plane, F is the bunch distribution function, $\delta\omega$ is the frequency shift of the oscillating particles, and $i\sigma$ is a vanishingly small term introduced in derivation to avoid singularities [2].

Given the coherent tune shift from an external source, one can use Eq. (1) to find the tune of the mode. Traditionally, to find Ω, one would solve Eq. (1) for all $\Delta\omega$. If one maps $Im[\Omega] = 0$ onto the complex plane of $\Delta\omega$, a threshold separating the stable and unstable states of the bunch is mapped, known as a Stability Diagram (SD). There are current techniques to measure stability diagrams for LD, though they have limitations [3]. We therefore investigate an alternative method to directly measure stability diagrams.

In this method of measuring the strength of LD, the polarity of a transverse feedback is reversed to excite a coherent mode in the beam. This creates an antidamper that produces a coupling impedance:

$$Z(\omega) \propto Ge^{i\phi}\delta(\omega) \qquad (2)$$

Where G is the antidamper gain and ϕ is the antidamper phase. The $\delta(\omega)$ shows that the antidamper kicks the bunch as a whole. The coupling impedance in Eq. (2) produces a coherent tune shift:

$$\Delta\omega \propto ge^{i\phi} \qquad (3)$$

Where g is the growth rate of the beam's centeroid position. One can independently change the gain and phase, making the antidamper a source of controlled impedance. Different combinations of phase and gain can be used to observe when the beam becomes unstable.

A schematic of a SD can be seen below in Fig. 1. G and ϕ combinations are changed until a growth rate is first observed, where the top-right subfigure of Fig. 1 shows the beam centroid position. The flat blue centroid position corresponds to G and ϕ before growth, where the growing red centroid position corresponds to G and ϕ after growth. The centroid position growth rate is used in Eq. (3) to map onto the complex $\Delta\omega$ plane at the red dot on the SD.

ISBN: 978-3-95450-247-9 ISSN: 2673-5490 doi: 10.18429/JACoW-IPAC2024-WEPR48

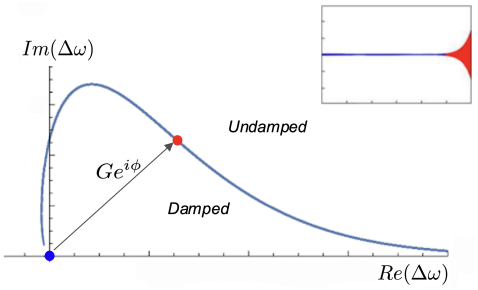

Figure 1: Stabilty Diagram, as it is obtained from an antidamper's gain G and phase ϕ [2] [3].

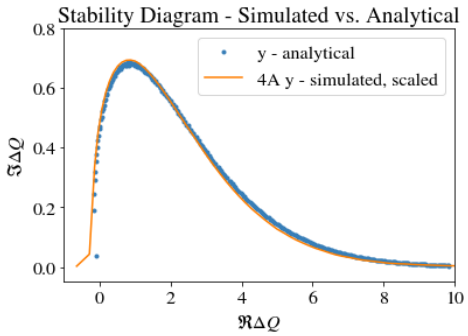

Figure 2: Simulated and analytical stability diagrams together, IOTA data is expected to follow these curves.

A proof-of-principle experiment of this method was performed at CERN [3]. This experiment inspired further research, where the IOTA experiment adds to this work by taking more phase measurements for a SD, to add quantitative results. The IOTA experiment also plans to investigate the impact of the machine's impedance, as well as investigate obtaining the beam distribution function from the SD, which has not been done this way before [2].

PREDICTIONS

There are both analytical and simulation predictions stability diagrams at IOTA. It is important to note that during data collection the source of LD was a string of octupoles, acting in the horizontal plane. The excitation from the antidamper and the turn-by-turn (tbt) data were both in the vertical plane. The theoretical predictions and the simulations were analyzed under these conditions. With these conditions, the normalized dispersion relation in Eq. (1) reduces to [2]:

$$\Delta\omega = \left[\int dJ_x \frac{F_x(J_x)}{\Omega - J_x + io}\right]^{-1} \tag{4}$$

The SD under these conditions was also simulated, using the simulation package Xsuite [4]. The simulations were run with each octupole set to a current of 4A. The resulting simulated SD, scaled by area to match the size of the normalized analytical SD, can be seen in Fig. 2 along with the normalized analytical SD. We expect to see an experimental SD resembling these curves.

METHODS

To create an antidamper as the source of controlled impedance, a transverse feedback was used, where the polarity was reversed to coherently excite the beam. The main experimental elements include a stripline kicker, two stripline BPMs, and a string of octupoles. The kicker and BPMs create the antidamper, where the octupoles supply the LD [5]. All of the octupoles were set to the same current of 4A, large enough to dominate nonlinear focusing in the ring.

In the antidamper system, the stripline kicker changes the antidamper gain. The two stripline BPMs can be combined to create a virtual bpm, giving adjustment of the phase advance of the antidamper. A schematic of the antidamper system in the IOTA ring is shown below in Fig. 3

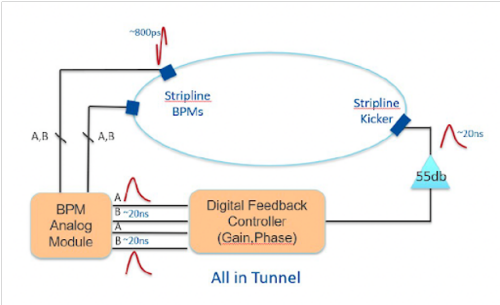

Figure 3: Schematic of antidamper elements in IOTA [5].

To collect data, we performed a sweep through kicker gains and BPM coefficients, where a change in BPM coefficients correspond directly to a change in phase advance. For each point in the SD, the phase (ϕ in Eq. (2)) was set, where for each phase, the kicker gain was swept through. The first growth rate per phase with an instability was the threshold growth rate, g. The growth rate and phase are the experimentally obtained values used in Eq. (3) to map out the SD.

EXPERIMENTAL RESULTS

To analyze the beam's growth rate per phase ϕ, the conversion between BPM coefficient and phase was performed. To obtain the phase from BPM coefficients, we swept through BPM coefficients where for each coefficient performed a Beam Transfer Function (BTF) of the lower and upper sidebands. The BTF excites the beam and reports frequency dependence of the beam response. The phases of maximum beam response are then used to calculate the total phase from virtual pickup to kicker per BPM coefficient.

The BTF ranges do not cover the full phase map, so data was taken at different additional turns in the ring before phase data was collected. This allowed for coverage of more phases for the SD. The data that is presented here corresponds to

ISBN: 978-3-95450-247-9 ISSN: 2673-5490 doi: 10.18429/JACoW-IPAC2024-WEPR48

no additional turn advances and two turn advances before phase data collection.

In the analysis, we obtain the threshold growth rate for each phase advance. An example of tbt centroid data at a kicker gain right after the first growth is shown in Fig. 4.

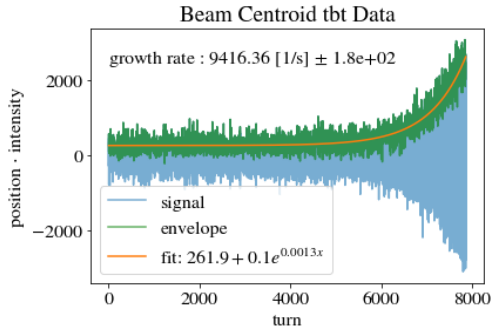

Figure 4: Tbt centroid data at the gain after the first growth.

For each first growth observed, the initial growth rate lies between the kicker gain with no growth and the kicker gain with first growth. To obtain a better estimate of the true threshold growth rate, a linear fit was performed on gain vs. growth rate. Looking closely at the linear relationship between gain and growth rate right between no growth and first growth, estimates of the first growth rate and the corresponding uncertainty were obtained. An example of the linear relationship between the gain and the growth rate is shown in Fig. 5.

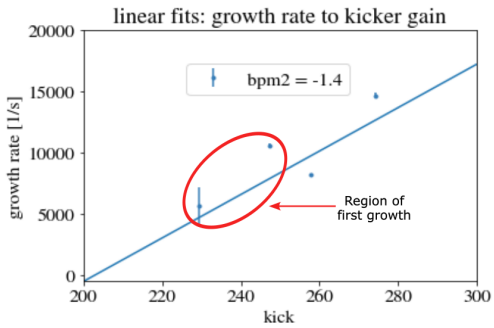

Figure 5: Kicker gain vs. growth rate. The area circled red locates the consecutive kicker gains where the threshold lies.

For each phase an estimated threshold growth rate was obtained and Eq. (3) was used to obtain $Re[\Delta\omega]$ and $Im[\Delta\omega]$ for the SD. The SDs for the no additional turn and two additional turn data can be seen in Fig. 6.

As can be seen in Fig. 6, there are some large uncertainties, outliers, and unexpected results in the data. There also seems to be a systematic rightward shift of the data. The error bar sources are mainly from the BTF step size and kick gain step size.

Additionally, it is important to note that the radiation damping was considered and found to be negligible compared to Landau damping during the measurements.

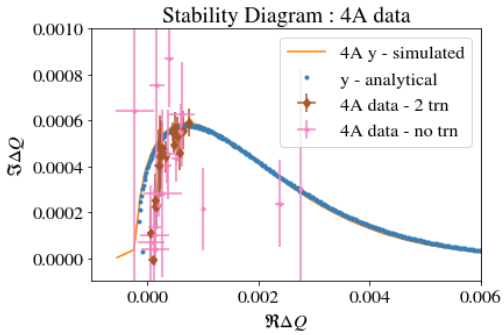

Figure 6: Total SD excluding major outliers.

CONCLUSIONS AND NEXT STEPS

The successes of the experiment include a significant increase in quantity of phase measurements. Additionally, the experimental data, simulation, and analytical predictions all qualitatively agree. This run for SD analysis also gave insight for proceeding in future runs.

Next steps for this experiment include steps for current data and future data. For current data, steps include investigating the systematic rightward shift and further investigating issues in phase-wrapping. The current results suggest an issue with the calculated phase and as the BTF data is the basis for the phase, it needs further study to fully understand and propagate the results. Additionally, next steps include obtaining the beam distribution function from the SD [2] and investigating the machine impedance's impact.

Goals for future electron runs include taking SD data for various octupole settings, obtaining more data for tails of the SDs, taking tighter BTF measurements, and directly measuring the amplitude detuning matrix. In Run 4 we were limited by the antidamper acting and measuring in one plane at a time, we would like to add capabilities to measure in both planes. Next steps for future proton runs include analyzing SDs with the impact of an electron lens and investigating LD in the regime with bunched beams and space charge.

ACKNOWLEDGEMENTS

We would like to thank the teams at the University of Chicago, Fermilab, and the IOTA/FAST collaboration for their support. We would also like to thank Alexey Burov for the many helpul discussions. This research is funded by the NSF Graduate Research Fellowships Program (GRFP). This manuscript has been authored by Fermi Research Alliance, LLC under Contract No. DE-AC02-07CH11359 with the U.S. Department of Energy, Office of Science, Office of High Energy Physics.

ISBN: 978-3-95450-247-9 ISSN: 2673-5490 doi: 10.18429/JACoW-IPAC2024-WEPR48

REFERENCES

[1] L. Palumbo and M. Migliorati, "Landau damping in particle accelerators," SAPIENZA University, Rome, Italy and INFN-LNF, unpublished, Sept. 2011.

[2] A. Burov, "Inverse stability problem in beam dynamics," *Phys. Rev. Accel. Beams*, vol. 26, p. 082801, Aug. 2023. doi:10.1103/PhysRevAccelBeams.26.082801

[3] S. Antipov *et al.*, "Proof-of-principle direct measurement of landau damping strength at the large hadron collider with an antidamper," *Phy. Rev. Lett.*, vol. 126, p. 164801, Apr. 2021. doi:10.1103/PhysRevLett.126.164801

[4] G. Iadarola *et al.*, "Xsuite: An Integrated Beam Physics Simulation Framework," in *Proc. HB'23*, Geneva, Switzerland, 2024, pp. 73–80. doi:10.18429/JACoW-HB2023-TUA2I1

[5] N. Eddy *et al.*, "Iota experiment nonlinear optics: Landau damping (niold)," Fermilab IOTA/FAST Experiment Proposal, unpublished, Apr. 2022.